European Journal of Medicinal Chemistry 89 (2015) 826–834

Contents lists available at ScienceDirect

European Journal of Medicinal Chemistry

journal homepage: http://www.elsevier.com/locate/ejmech

Design, synthesis and biological evaluation of 6-(nitroimidazole-1*H*-alkyloxyl)-4-anilinoquinazolines as efficient EGFR inhibitors exerting cytotoxic effects both under normoxia and hypoxia

Weiyan Cheng, Shijun Zhu, Xiaodong Ma, Ni Qiu, Peng Peng, Rong Sheng*, Yongzhou Hu*

Zhejiang Province Key Laboratory of Anti-Cancer Drug Research, College of Pharmaceutical Sciences, Zhejiang University, Hangzhou 310058, China

ARTICLE INFO

Article history:
Received 5 August 2014
Received in revised form
27 October 2014
Accepted 5 November 2014
Available online 6 November 2014

Keywords:
EGFR inhibitor
4-Anilinoquinazoline
Nitroimidazole
Normoxia
Hypoxia

ABSTRACT

A series of novel 6-(nitroimidazole-1*H*-alkyloxyl)-4-anilinoquinazoline derivatives (**15a**–**15r**) were designed, synthesized and evaluated as efficient EGFR inhibitors through introduction of hypoxia activated nitroimidazole moiety into the quinazoline scaffold of EGFR inhibitors. The majority of these newly synthesized compounds exhibited comparable EGFR inhibitory activities to gefitinib and moderate to excellent anti-proliferative activities against HT-29 cells under normoxia and hypoxia. The most promising compound **15c** displayed the IC_{50} value of 0.47 nM against EGFR kinase and excellent cytotoxic effect against HT-29 cells under normoxia and hypoxia with the IC_{50} values of 2.21 μM and 1.62 μM, respectively. The mimic reductive activation study revealed that compound **15c** exerted reductive activation properties under hypoxia, which were consistent with the *in vitro* metabolic study, wherein **15c** was easily reductive activated under hypoxia and much more stable under normoxia. All these results suggested that **15c** was a potential cancer therapeutic agent both under normoxia and hypoxia and was worth of further development.

1. Introduction

As a member of the HER family, epidermal growth factor receptor (EGFR) plays a vital role in the cellular signaling transduction processes [1]. The over-expression of EGFR has been observed in many solid tumors, such as colon [2], ovarian [3], and non-small cell lung cancer (NSCLC) [4]. Therefore, EGFR inhibition has been developed as one of the most efficient strategies for cancer therapy. In the past few years, more than 20 EGFR inhibitors have been advanced into clinical trials, and four 4-anilinoquinazoline derivatives, termed as gefitinib (**1**), erlotinib (**2**), lapatinib (**3**), and afatinib (**4**), have been approved by FDA for the treatment of NSCLC, pancreatic cancer and advanced breast cancer (Fig. 1) [5].

As an inevitable circumstance in most solid tumors, hypoxia is responsible for the resistance to radiotherapy and chemotherapy and presents a tremendous challenge to cancer therapy [6]. Especially, the expression of EGFR is up-regulated when tumors are under hypoxia, which is closely related to tumor survival [7,8]. Therefore, design and development of EGFR inhibitors with potency to overcome EGFR up-regulation under hypoxia may exert better effects for cancer therapy.

The specific hypoxic micro-environment of tumor cells also makes it as an attractive and exploitable therapeutic target. 2-Nitroimidazole derivatives have been developed as hypoxia activated radio-sensitization and chemotherapy agents since 1960s [9]. Under hypoxia, the 2-nitroimidazole moiety was reduced by nitroreductase to yield reactive radicals, which could deplete tumor endogenous protective agents such as glutathione (GSH) to make tumors be sensitive to radiotherapy [10]. Moreover, the irreversibly binding of reactive radicals to the cellular protein and nucleic acids makes them accumulate therein and exert cytotoxic effects [11]. Up to now, several radioactive 2-nitroimidazole derivatives have been advanced into clinical trials for the noninvasive assessment of hypoxia in cancer, including [^{18}F]FMISO (**5**), [^{18}F]FAZA (**6**) and [^{18}F]HX4 (**7**) (Fig. 1) [12,13]. Based on the above reports, we envisioned that EGFR inhibitors containing hypoxia activated pharmacophore may exert efficient antitumor activities both under normoxia and hypoxia.

The crystal structures of 4-anilinoquinazoline–EGFR complexes reveal that the quinazoline scaffold confers an H-bond interaction to the hinge domain of the kinase and the aniline moiety inserts into the hydrophobic pocket, which are crucial for EGFR inhibitory

* Corresponding authors.
E-mail addresses: shengr@zju.edu.cn (R. Sheng), huyz@zju.edu.cn (Y. Hu).

http://dx.doi.org/10.1016/j.ejmech.2014.11.010
0223-5234/

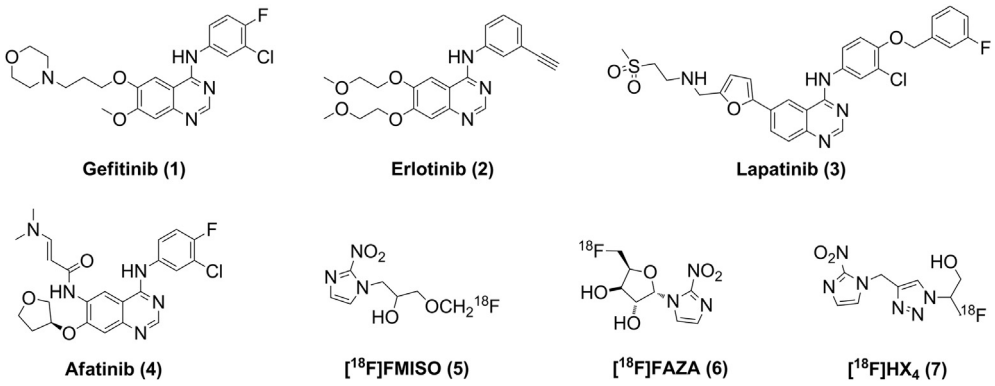

Fig. 1. Structures of selected EGFR inhibitors and 2-nitroimidazole derivatives.

activity. The side chains at the *C*-6 and *C*-7 positions are projected to the solvent portion which exerts good compatibility for long ether chains or other moieties [14–17] (Fig. 2). Therefore, a series of novel EGFR inhibitors were designed and synthesized through incorporating 2-nitroimidazole and its analogue 2-methyl-5-nitroimidazole into the *C*-6 position of the 4-anilinoquinazoline scaffold. Different kinds of anilines from gefitinib, erlotinib, lapatinib and other advanced EGFR inhibitor were employed to the *C*-4 position of the quinazoline template, as well as the length of linker between the nitroimidazole and quinazoline was probed for the SAR study (Fig. 2).

2. Results and discussion

2.1. Chemistry

The synthetic route to compounds **15a**–**15r** was displayed in Scheme 1. Compounds **9a**–**9e** were prepared via alkylation of 2-nitroimidazole (**8**) with α, ω-dibromoalkane in the presence of potassium carbonate, and compounds **11a**–**11c** were obtained in a similar way by using 2-methyl-5-nitroimidazole (**10**) as the start material. Condensation of compound **12** with substituted anilines afforded 4-anilinoquinazoline derivatives **13a**–**13d** [18], followed by de-acetylation with aqueous ammonia provided **14a**–**14d** as the key intermediates. Finally, reaction of **14a**–**14d** with **9a**–**9e** or **11a**–**11c** in the presence of potassium carbonate furnished title compounds **15a**–**15r**.

2.2. In vitro EGFR inhibitory activity

The EGFR inhibitory activities of compounds **15a**–**15r** were evaluated using a well established Z′-Lyte assay and gefitinib was employed as the positive control [19]. As shown in Table 1, most of the tested compounds (**15b**–**15j**, **15q**, and **15r**) exhibited potent EGFR inhibitory activities with the IC_{50} values ranging from 0.32 to 1.18 nM, which were comparable to that of gefitinib (IC_{50} = 0.45 nM). The introduction of the bulky substituents on aniline resulted in a dramatic decrease in activity. For instance, compounds **15k**–**15n** only demonstrated EGFR inhibition with the IC_{50} values ranging from 15.1 to 51.2 nM, which were more than 30 fold less potent than gefitinib. Other compounds with small substituents on aniline demonstrated favorable inhibitory activity with the IC_{50} values ranging from 0.32 to 4.90 nM, indicating that bulky moiety on aniline may prevent the aniline from adapting the hydrophobic pocket of EGFR kinase. The length of linker between the imidazole and quinazoline also significantly affected the activities. The compromised EGFR inhibitory activities of compound **15a**, **15b**, **15o** and **15p** compared to **15c** and **15q** indicated that longer linkers (n = 3–5) were more favorable than shorter ones (n = 1–2).

2.3. In vitro anti-proliferative activity

The human colorectal adenocarcinoma HT-29 cells were widely used to evaluate the biological activities of the hypoxia-activated drugs, and this kind of cells also expressed high levels of EGFR [20–23]. Therefore, the anti-proliferative activities of compounds **15a**–**15r** were evaluated against HT-29 cells under normoxia and hypoxia. As shown in Table 1, most of these compounds demonstrated moderate to excellent anti-proliferative activities. Especially, five compounds (**15c**, **15i**, **15j**, **15l**, and **15m**) were more potent than gefitinib both under normoxia (IC_{50} values: 1.87–3.55 μM) and hypoxia (IC_{50} values: 1.36–3.46 μM). Gefitinib exhibited less potent anti-proliferative activity under hypoxia (IC_{50} = 5.21 μM) than normoxia (IC_{50} = 3.63 μM), probably because the over-expression of EGFR made tumors be more resistant under hypoxia. For the newly synthesized compounds, most of them (**15a**–**15i** and **15m**–**15p**) exhibited comparable or more potent anti-proliferative activities under hypoxia than under normoxia. We deduced that the cytotoxicities contributed by the reductive activation of these compounds were partly offset by the increased

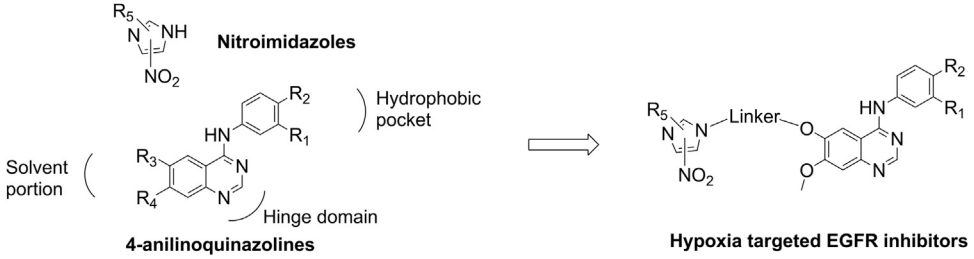

Fig. 2. Design of new EGFR inhibitors containing hypoxia activated pharmacophores.

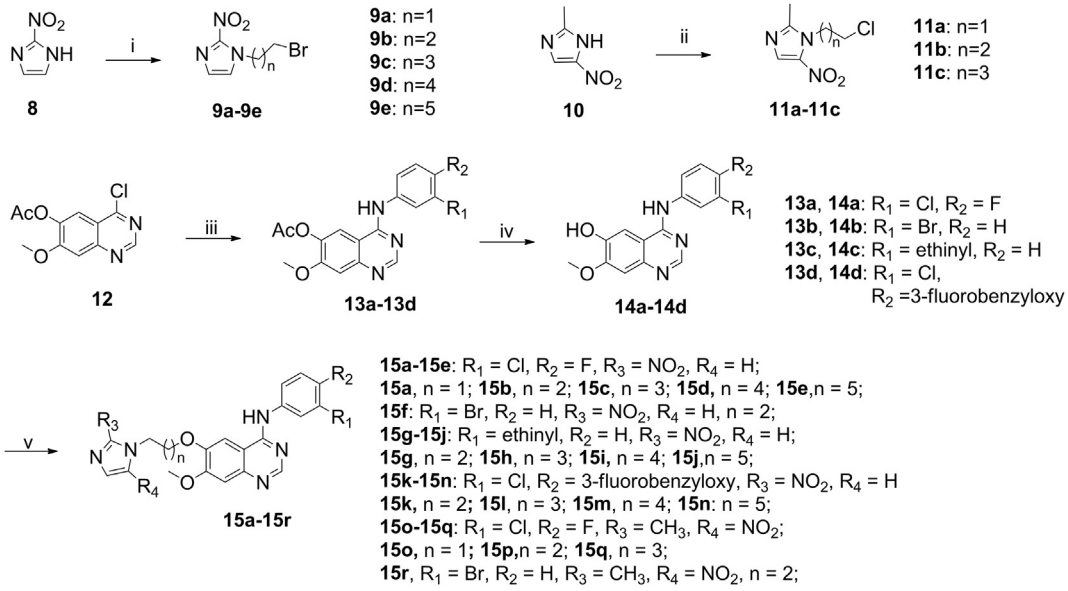

Scheme 1. Synthesis of **15a**–**15r**. Reagents and conditions: (i) α, ω-dibromoalkane, K_2CO_3, DMF, 60 °C, 4 h. (ii)α-bromo-ω-chloro-alkane, K_2CO_3, DMF, 60 °C, 4 h. (iii) substituted aniline, isopropanol, reflux, 1 h; (iv) ammonia/methanol, rt, 3 h; (v) **9a**–**9e**, **11a**–**11c**, K_2CO_3, DMF, 80 °C, 5 h.

vitalities of the HT-29 cells under hypoxia, and this led to the relatively less obvious difference in the IC_{50} values between normoxia and hypoxia.

Compounds with 2-nitroimidazole moieties exhibited more potent anti-proliferative activities than 2-methyl-5-nitroimidazole-containing ones (**15b** vs **15p**, **15c** vs **15q**, and **15f** vs **15r**), indicating that 2-nitroimidazole was a more favorable hypoxia-activated moiety [24]. In addition, although compound **15l** and **15m** displayed compromised EGFR inhibitory activities (IC_{50} = 28.5, 51.2 nM, respectively) compared to gefitinib, they demonstrated excellent anti-proliferative activities with the IC_{50} values of 1.87 and 3.09 μM under normoxia, 2.07 and 1.36 μM under

Table 1
In vitro EGFR inhibitory and anti-proliferative activities of compounds **15a**–**15r**.

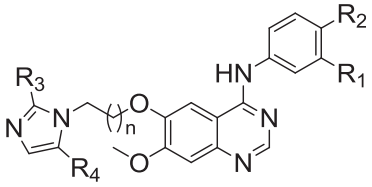

Compd.	R_1	R_2	*n*	R_3	R_4	EGFR[a] (IC_{50}, nM)	HT-29 (IC_{50}, μM)[a]	
							Normoxia	Hypoxia
15a	Cl	F	1	NO_2	H	3.05 ± 0.52	>50	10.02 ± 2.56
15b	Cl	F	2	NO_2	H	0.89 ± 0.31	8.39 ± 2.32	7.17 ± 1.87
15c	Cl	F	3	NO_2	H	0.47 ± 0.10	2.21 ± 0.54	1.62 ± 0.39
15d	Cl	F	4	NO_2	H	0.51 ± 0.14	17.58 ± 4.12	5.59 ± 1.08
15e	Cl	F	5	NO_2	H	0.32 ± 0.11	12.89 ± 2.49	9.81 ± 1.34
15f	Br	H	2	NO_2	H	0.66 ± 0.13	4.48 ± 0.68	4.01 ± 0.57
15g	Ethynyl	H	2	NO_2	H	1.08 ± 0.34	5.55 ± 1.06	5.53 ± 0.89
15h	Ethynyl	H	3	NO_2	H	0.56 ± 0.17	10.08 ± 2.34	6.90 ± 1.02
15i	Ethynyl	H	4	NO_2	H	0.49 ± 0.23	3.55 ± 0.78	3.05 ± 0.63
15j	Ethynyl	H	5	NO_2	H	0.50 ± 0.12	2.93 ± 0.82	3.46 ± 0.91
15k	Cl	3-Fluorobenzyloxy	2	NO_2	H	38.3 ± 4.83	15.48 ± 3.23	20.00 ± 3.31
15l	Cl	3-Fluorobenzyloxy	3	NO_2	H	28.5 ± 6.65	1.87 ± 0.73	2.07 ± 1.02
15m	Cl	3-Fluorobenzyloxy	4	NO_2	H	51.2 ± 12.43	3.09 ± 0.93	1.36 ± 0.45
15n	Cl	3-Fluorobenzyloxy	5	NO_2	H	15.1 ± 4.18	>50	24.31 ± 3.34
15o	Cl	F	1	CH_3	NO_2	4.90 ± 0.76	>50	>50
15p	Cl	F	2	CH_3	NO_2	3.43 ± 0.54	23.24 ± 4.23	11.52 ± 2.31
15q	Cl	F	3	CH_3	NO_2	0.53 ± 0.21	8.21 ± 3.25	9.98 ± 2.03
15r	Br	H	2	CH_3	NO_2	1.18 ± 0.13	15.72 ± 4.51	5.41 ± 1.32
Gefitinib	–	–	–	–	–	0.45 ± 0.12	3.63 ± 0.58	5.21 ± 0.93
TPZ[b]	–	–	–	–	–	–	>50	9.45 ± 2.81

[a] The data were means from at least three independent experiments.
[b] TPZ: Tirapazamine.

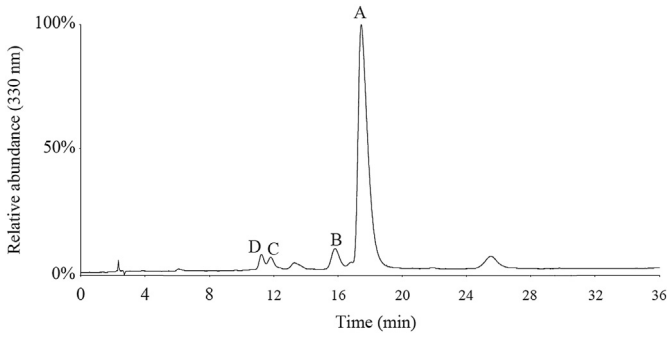

Fig. 3. The HPLC chromatograms of products in the mimic reductive activation of compound **15c**.

hypoxia, respectively. The most promising compound **15c** displayed extraordinary cytotoxic activities against HT-29 cells under both normoxia and hypoxia with the IC_{50} values of 2.21 μM and 1.62 μM, respectively, and it was selected for further study.

2.4. Mimic the reductive activation of compound 15c

As reported, the 2-nitroimidazole derivatives may experience reductive activation under tumor hypoxia and zinc dust was used to mimic this process [25,26]. To confirm this speculation, compound **15c** was chosen to react with zinc dust and cysteine was used to catch the produced reactive radicals [27,28]. The reaction was carried out in the phosphate buffer saline at 37 °C under hypoxia, and the resulting mixture was detected by HPLC-Q-ToF-MS. As shown in Fig. 3, several peaks were appeared within the retention time of 36 min. Among them, peak A (m/z = 457.1569) was the main product of the reaction and was confirmed as the 2-aminoimidazole derivative. The appearance of peak B (m/z = 695.1663) and peak C (m/z = 576.1618) indicated that two or one molecular cysteines were bounded to one reactive radical, respectively. The peak D (m/z = 391.1349) was deduced as the degeneration product of the reactive radical.

According to the LC–MS results of mimic reduction reaction of **15c**, we deduced that compound **15c** experienced the following reductive process (Fig. 4).

2.5. Metabolic stability of compound 15c under normoxia and hypoxia

To further evaluate the metabolic stability of compound **15c** under normoxia and hypoxia, it was incubated with mouse liver microsomes using NADPH as the activator [29] and gefitinib as the reference. As shown in Fig. 5, gefitinib exerted similar metabolic stability profile under normoxia and hypoxia, with more than 90% remained after 30 min incubation. While for compound **15c**, about 70% remained under normoxia and less than 10% remained under hypoxia. These results indicated that compound **15c** was relatively stable under normoxia and could be easily metabolic activation under hypoxia.

2.6. Molecular docking study

To predict the possible binding mode of this series of compounds with EGFR, the docking study of compound **15c** with EGFR kinase (PDB ID: 2ITY) was performed using gefitinib as a comparison. As illustrated in Fig. 6, compound **15c** favorably fitted into EGFR in a similar way to gefitinib, the 3-chloro-4-fluoro-aniline moiety inserted into the hydrophobic pocket formed by Met766, Glu762, Lys745 and Leu788, and the fluorine atom interacted with Lys745 through a hydrogen bond with a distance of 2.92 Å. Another hydrogen bond was formed between Met793 and *N*-1 of the quinazoline with a distance of 2.99 Å. As expected, the 2-nitroimidazole side chain was positioned at the solvent portion of the kinase which was similar to the morpholine moiety of gefitinib.

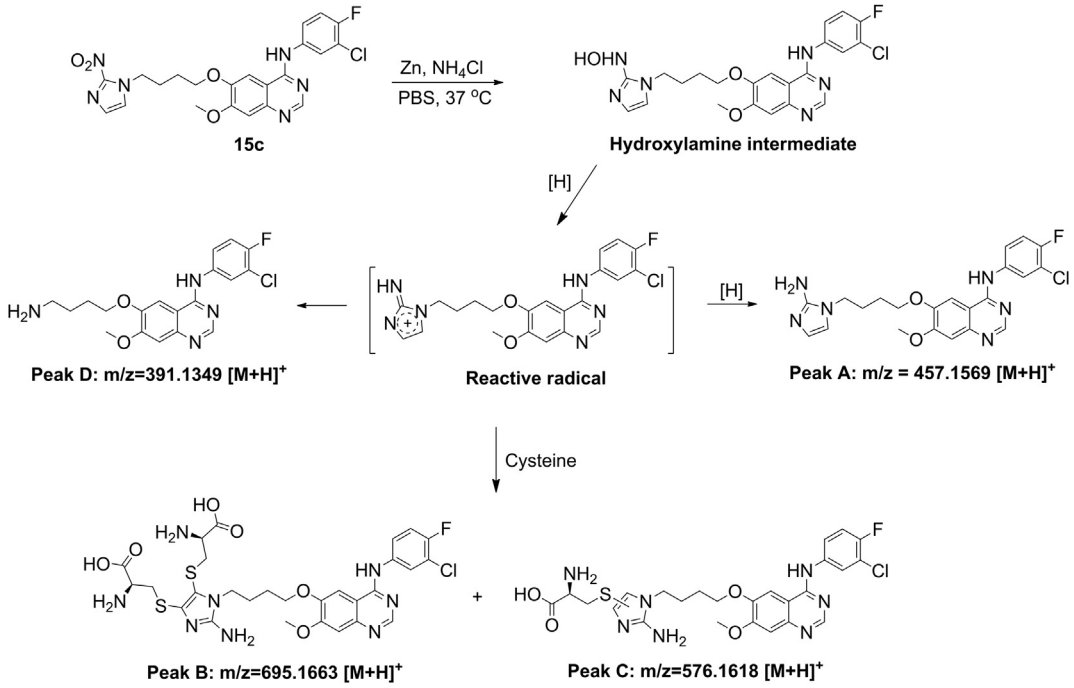

Fig. 4. The proposed reductive activation process of compound **15c**.

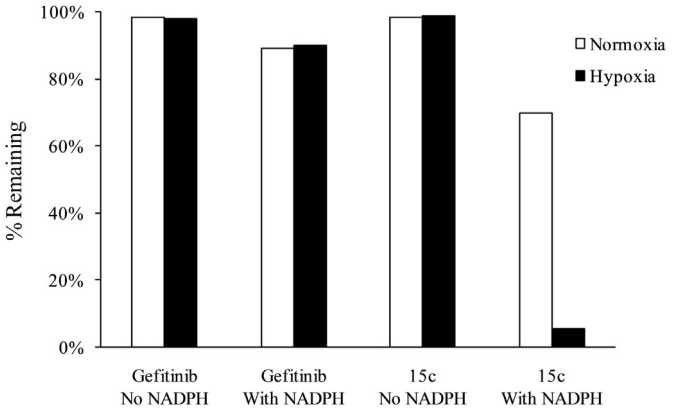

Fig. 5. The percentage of intact compound **15c** and gefitinib after 30 min of *in vitro* metabolism reaction.

3. Conclusion

To overcome the EGFR up-regulation under tumor hypoxia, a novel series of EGFR inhibitors were synthesized by incorporating the nitroimidazole moieties into the *C*-6 position of the 4-anilinoquinazolines with proper linkers. Most of the compounds exhibited excellent EGFR inhibitory activities *in vitro* and the SARs revealed that bulky substituents on aniline and short linkers between nitroimidazole and quinazoline were detrimental to the enzymatic activity. The molecular docking study of **15c** with EGFR has revealed that it could fit well into EGFR kinase in a similar way to gefitinib. Most of these compounds demonstrated moderate to excellent anti-proliferative activities against HT-29 cells under normoxia and hypoxia. The most promising compound **15c** exhibited excellent anti-proliferative activities with the IC_{50} values of 2.21 and 1.62 μM under normoxia and hypoxia, respectively, which were more potent than that of gefitinib. The mimic reductive activation study revealed that compound **15c** could be reduced to generate reactive radicals and covalently bound to nucleophiles under hypoxia. Moreover, the metabolic stability study indicated that compound **15c** could be easily reductive activated under hypoxia. All these results demonstrated that compound **15c** was a potential cancer therapeutic agent under normoxia as well as hypoxia and was worth of further development.

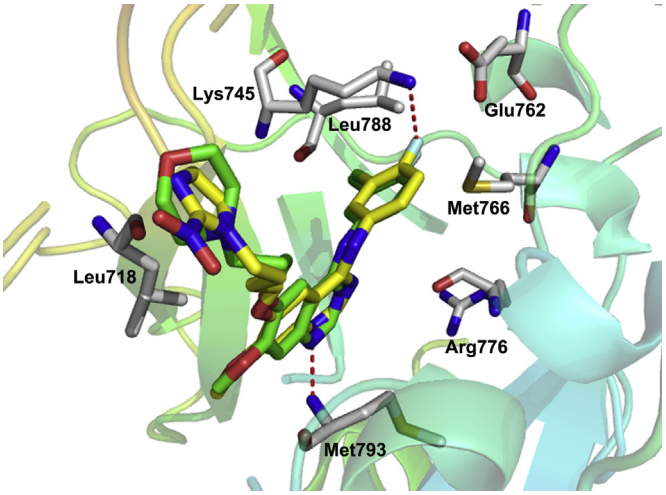

Fig. 6. The docked poses of compound **15c** (*C*: yellow; *N*: blue; *O*: red) or gefitinib (*C*: green; *N*: blue; *O*: red) at the ATP binding cleft of EGFR kinase. (For interpretation of the references to colour in this figure legend, the reader is referred to the web version of this article.)

4. Experimental

4.1. Chemistry

4.1.1. General methods/instruments

Melting points were recorded on a B-540 Büchi melting-point apparatus and are uncorrected, ^{1}H NMR were recorded on a BRUKER AVIII 500 MHz or AVII 400 MHz and ^{13}C NMR were recorded on a BRUKER AVII 100 MHz spectrometer with TMS as the internal standard. Proton chemical shifts are expressed in parts per million (ppm) and coupling constants in Hz. Mass spectra (ESI-MS) were performed on a Finnigan LCQ Deca XP ion trap mass spectrometry. High resolution mass spectra were measured on an Agilent 1290 HPLC-6224 Time of Fight Mass Spectrometer.

4.1.2. General synthetic procedure of nitroimidazole derivatives (**9a**–**9e**, **11a**–**11c**)

Dibromo-alkane (0.04 mol) was added to a stirred mixture of nitroimidazole derivative (**8** or **10**, 0.01 mol) and potassium carbonate (1.38 g, 0.02 mol) in DMF (5 mL). The mixture was heated to 60 °C and stirred for about 4 h. After cooling to room temperature, the mixture was filtered and the filtrate was concentrated to dryness. The residue was purified by silica gel column chromatography to get pure **9a**–**9e** and **11a**–**11c**.

*4.1.2.1. 1-(2-Bromoethyl)-2-nitro-1H-imidazole (**9a**).* Yellow solid, yield: 87%, mp: 62–64 °C.

*4.1.2.2. 1-(3-Bromopropyl)-2-nitro-1H-imidazole (**9b**).* Yellow oil, yield: 82%. ^{1}H NMR (500 MHz, $CDCl_3$) δ 7.21 (s, 1H), 7.17 (s, 1H), 4.62 (t, J = 6.5 Hz, 2H), 3.38 (t, J = 6.0 Hz, 2H), 2.45–2.38 (m, 2H). ESI-MS m/z: 234 $[M+H]^+$.

*4.1.2.3. 1-(4-Bromobutyl)-2-nitro-1H-imidazole (**9c**).* Yellow oil, yield: 86%. ^{1}H NMR (500 MHz, $CDCl_3$) δ 7.15 (s, 1H), 7.11 (s, 1H), 4.46 (t, J = 7.5 Hz, 2H), 3.42 (t, J = 6.5 Hz, 2H), 2.08–2.00 (m, 2H), 1.95–1.88 (m, 2H). ESI-MS m/z: 248 $[M+H]^+$.

*4.1.2.4. 1-(5-Bromopentyl)-2-nitro-1H-imidazole (**9d**).* Yellow oil, yield: 82%. ^{1}H NMR (500 MHz, $CDCl_3$) δ 7.14 (s, 1H), 7.10 (s, 1H), 4.42 (t, J = 7.5 Hz, 2H), 3.40 (t, J = 6.5 Hz, 2H), 1.93–1.84 (m, 4H), 1.55–1.49 (m, 2H). ESI-MS m/z: 262 $[M+H]^+$.

*4.1.2.5. 1-(6-Bromohexyl)-2-nitro-1H-imidazole (**9e**).* Yellow oil, yield: 89%. ^{1}H NMR (500 MHz, $CDCl_3$) δ 7.14 (s, 1H), 7.08 (s, 1H), 4.41 (t, J = 7.5 Hz, 2H), 3.40 (t, J = 7.0 Hz, 2H), 1.91–1.81 (m, 4H), 1.53–1.47 (m, 2H), 1.41–1.35 (m, 2H). ESI-MS m/z: 276 $[M+H]^+$.

*4.1.2.6. 1-(2-Chloroethyl)-2-methyl-5-nitro-1H-imidazole (**11a**).* White solid, yield: 74%, mp: 73–75 °C (lit. 78–79 °C) [30].

*4.1.2.7. 1-(3-Chloropropyl)-2-methyl-5-nitro-1H-imidazole (**11b**).* White solid, yield: 78%, mp: 61–63 °C (lit. 65–67 °C) [31].

*4.1.2.8. 1-(4-Chlorobutyl)-2-methyl-5-nitro-1H-imidazole (**11c**).* White solid, yield: 79%, mp: 67–69 °C. ^{1}H NMR (500 MHz, $CDCl_3$) δ 7.69 (s, 1H), 3.97 (t, J = 7.5 Hz, 2H), 3.58 (t, J = 6.5 Hz, 2H), 2.43 (s, 3H), 2.03–1.93 (m, 2H), 1.87–1.79 (m, 2H). ESI-MS m/z: 218 $[M+H]^+$.

*4.1.3. General synthetic procedure of 4-anilinoquinazoline derivatives (**14a**–**14d**)*

Compound **12** [18] (10.0 mmol) and substituted aniline (15.0 mmol) were mixed in isopropanol (10.0 mL) and refluxed for 1 h. After cooling to room temperature, the white solid was filtered to get compounds **13a**–**13d** without further purification. Compounds **13a**–**13d** was added to the mixture of methanol (15.0 mL) and 25% ammonia (2.0 mL) and stirred for 3–4 h at room temperature. The solid was filtered and washed with chilled methanol and dried in vacuum to obtain **14a**–**14d**.

*4.1.4. General synthetic procedure of final compounds (**15a**–**15r**)*

Nitroimidazole derivatives (**9a**–**9e** and **11a**–**11c**, 0.18 mmol) were added to a mixture of 4-anilinoquinazoline derivatives (**14a**–**14d**, 0.15 mmol) and potassium carbonate (0.3 mmol) in DMF (3.0 mL). The reaction mixture was heated to 80 °C and stirred for about 5 h. After cooling to room temperature, the mixture was filtered and the filtrate was concentrated to dryness. H_2O (15 mL) was added to the residue and extracted with ethyl acetate (15 mL × 3). The combined organic layer was washed with brine, dried over anhydrous Na_2SO_4. The solvent was evaporated to dryness and the residue was purified with silica gel chromatography to give title compounds **15a**–**15r**.

*4.1.4.1. N-(3-chloro-4-fluorophenyl)-7-methoxy-6-(2-(2-nitro-1H-imidazol-1-yl)ethoxy)quinazolin-4-amine (**15a**).* White solid, yield: 43%, mp: 229–231 °C. ^{1}H NMR (400 MHz, DMSO-d_6) δ 9.52 (s, 1H), 8.50 (s, 1H), 8.08–8.13 (m, 1H), 7.82 (s, 1H), 7.80–7.73 (m, 1H), 7.71 (s, 1H), 7.44 (t, J = 9.2 Hz, 1H), 7.22 (s, 1H), 7.18 (s, 1H), 4.95 (t, J = 5.2 Hz, 2H), 4.51 (t, J = 5.2 Hz, 2H), 3.91 (s, 3H). ^{13}C NMR (100 MHz, DMSO-d_6) δ 156.3, 154.6, 153.4 (d, J_{C-F} = 242.7 Hz), 152.1, 147.6, 147.5, 145.2, 136.9 (d, J_{C-F} = 2.7 Hz), 128.5, 127.9, 123.7, 122.6 (d, J_{C-F} = 6.8 Hz), 119.0 (d, J_{C-F} = 18.3 Hz), 116.8 (d, J_{C-F} = 21.5 Hz), 108.8, 107.7, 103.4, 67.6, 56.2, 48.6. ESI-MS m/z: 459 $[M+H]^+$. HRMS (ESI): m/z calcd for $(C_{20}H_{16}ClFN_6O_4 + H)^+$: 459.0984; found: 459.0986.

*4.1.4.2. N-(3-chloro-4-fluorophenyl)-7-methoxy-6-(3-(2-nitro-1H-imidazol-1-yl)propoxy)quinazolin-4-amine (**15b**).* White solid, yield: 62%, mp: 199–201 °C. ^{1}H NMR (500 MHz, DMSO-d_6) δ 11.55 (s, 1H), 8.89 (s, 1H), 8.36 (s, 1H), 8.00–8.03 (m, 1H), 7.75–7.70 (m, 2H), 7.55 (t, J = 9.0 Hz, 1H), 7.31 (s, 1H), 7.17 (d, J = 1.0 Hz, 1H), 4.62 (t, J = 6.5 Hz, 2H), 4.30 (t, J = 6.0 Hz, 2H), 3.98 (s, 3H), 2.43–2.37 (m, 2H). ^{13}C NMR (100 MHz, DMSO-d_6) δ 156.1, 154.6, 153.2 (d, J_{C-F} = 242.8 Hz), 152.7, 147.9, 146.9, 144.7, 136.7 (d, J_{C-F} = 2.7 Hz), 127.9, 127.8, 123.5, 122.3 (d, J_{C-F} = 6.9 Hz), 118.8 (d, J_{C-F} = 18.3 Hz), 116.5 (d, J_{C-F} = 21.5 Hz), 108.6, 107.2, 102.9, 66.1, 55.9, 47.0, 29.1. ESI-MS m/z: 473 $[M+H]^+$. HRMS (ESI): m/z calcd for $(C_{21}H_{18}ClFN_6O_4 + H)^+$: 473.1140; found: 473.1147.

*4.1.4.3. N-(3-chloro-4-fluorophenyl)-7-methoxy-6-(4-(2-nitro-1H-imidazol-1-yl)butoxy)quinazolin-4-amine (**15c**).* White solid, yield: 51%, mp: 188–190 °C. ^{1}H NMR (500 MHz, DMSO-d_6) ^{1}H NMR (500 MHz, DMSO-d_6) δ 9.53 (s, 1H), 8.50 (s, 1H), 8.11–8.13 (m, 1H), 7.85–7.73 (m, 3H), 7.45 (t, J = 9.5 Hz, 1H), 7.21 (s, 2H), 4.52 (t, J = 7.0 Hz, 2H), 4.19 (t, J = 6.0 Hz, 2H), 3.94 (s, 3H), 2.07–1.98 (m, 2H), 1.89–1.80 (m, 2H). ^{13}C NMR (100 MHz, DMSO-d_6) δ 158.2, 156.5, 155.0 (d, J_{C-F} = 243.3 Hz), 149.4, 148.44, 144.6, 135.1, 134.2 (d, J_{C-F} = 2.8 Hz), 127.9, 127.8, 126.7, 125.4 (d, J_{C-F} = 7.3 Hz), 119.0 (d, J_{C-F} = 18.6 Hz), 116.7 (d, J_{C-F} = 22.0 Hz), 107.3, 105.2, 99.5, 69.3, 56.5, 49.1, 26.5, 25.1. ESI-MS m/z: 487 $[M+H]^+$. HRMS (ESI): m/z calcd for $(C_{22}H_{20}ClFN_6O_4 + H)^+$: 487.1297; found: 487.1297.

*4.1.4.4. N-(3-chloro-4-fluorophenyl)-7-methoxy-6-((5-(2-nitro-1H-imidazol-1-yl)pentyl)oxy)quinazolin-4-amine (**15d**).* Yellow solid, yield: 68%, mp: 180–182 °C. ^{1}H NMR (500 MHz, DMSO-d_6) δ 9.51 (s, 1H), 8.48 (s, 1H), 8.09–8.11 (m, 1H), 7.81–7.74 (m, 2H), 7.71 (d, J = 0.5 Hz, 1H), 7.43 (t, J = 9.0 Hz, 1H), 7.20–7.17 (m, 2H), 4.42 (t, J = 7.0 Hz, 2H), 4.12 (t, J = 6.5 Hz, 2H), 3.91 (s, 3H), 1.92–1.81 (m, 4H), 1.50–1.44 (m, 2H). ^{13}C NMR (100 MHz, DMSO-d_6) δ 156.2, 154.7, 152.8, 153.4 (d, J_{C-F} = 242.5 Hz), 152.8, 148.5, 147.2, 144.8 (d, J_{C-F} = 2.7 Hz), 137.0 (d, J_{C-F} = 3.0 Hz), 128.1 (2), 123.7, 122.5 (d, J_{C-F} = 6.9 Hz), 119.0 (d, J_{C-F} = 18.5 Hz), 116.7 (d, J_{C-F} = 21.5 Hz), 109.0, 107.5, 102.7, 68.8, 56.1, 49.5, 29.8, 28.3, 22.8. ESI-MS m/z: 501 $[M+H]^+$. HRMS (ESI): m/z calcd for $(C_{23}H_{22}ClFN_6O_4 + H)^+$: 501.1453; found: 501.1459.

*4.1.4.5. N-(3-chloro-4-fluorophenyl)-7-methoxy-6-((6-(2-nitro-1H-imidazol-1-yl)hexyl)oxy)quinazolin-4-amine (**15e**).* Yellow solid, yield: 66%, mp: 160–162 °C. ^{1}H NMR (500 MHz, DMSO-d_6) δ 9.51 (s, 1H), 8.48 (s, 1H), 8.09–8.11 (m, 1H), 7.81–7.74 (m, 2H), 7.69 (d, J = 0.5 Hz, 1H), 7.43 (t, J = 9.0 Hz, 1H), 7.18 (s, 1H), 7.16 (d, J = 0.5 Hz, 1H), 4.38 (t, J = 7.5 Hz, 2H), 4.11 (t, J = 6.5 Hz, 2H), 3.92 (s, 3H), 1.87–1.77 (m, 4H), 1.53–1.47 (m, 2H), 1.41–1.34 (m, 2H). ^{13}C NMR (100 MHz, DMSO-d_6) δ 156.0, 153.2 (d, J_{C-F} = 242.7 Hz), 152.5, 148.4, 146.8, 144.5, 136.8 (d, J_{C-F} = 3.1 Hz), 127.8, 127.8, 123.5, 122.4 (d, J_{C-F} = 6.7 Hz), 118.8 (d, J_{C-F} = 18.3 Hz), 116.5 (d, J_{C-F} = 21.8 Hz), 108.7, 107.2, 102.4, 68.6, 55.9, 49.3, 29.7, 28.5, 25.6, 25.1. ESI-MS m/z: 515 $[M+H]^+$. HRMS (ESI): m/z calcd for $(C_{24}H_{24}ClFN_6O_4 + H)^+$: 515.1610; found: 515.1612.

*4.1.4.6. N-(3-bromophenyl)-7-methoxy-6-(3-(2-nitro-1H-imidazol-1-yl)propoxy)quinazolin-4-amine (**15f**).* White solid, yield: 48%, mp: 111–113 °C. ^{1}H NMR (500 MHz, MeOD) δ 8.73 (s, 1H), 8.01 (t, J = 2.0 Hz, 1H), 7.99 (s, 1H), 7.72–7.69 (m, 1H), 7.53 (d, J = 1.0 Hz, 1H), 7.50–7.48 (m, 1H), 7.40 (t, J = 8.0 Hz, 1H), 7.22 (s, 1H), 7.13 (d, J = 1.0 Hz, 1H), 4.79 (t, J = 6.5 Hz, 2H), 4.38–4.28 (m, 2H), 4.06 (s, 3H), 2.59–2.46 (m, 2H). ^{13}C NMR (100 MHz, DMSO-d_6) δ 158.5, 156.8, 149.4, 148.8, 145.0, 138.8, 135.7, 130.8, 129.1, 128.1 (2), 127.5, 123.9, 121.3, 107.5, 105.4, 99.8, 67.3, 56.7, 47.1, 29.2. ESI-MS m/z: 501 $[M+H]^+$. HRMS (ESI): m/z calcd for $(C_{21}H_{19}BrN_6O_4 + H)^+$: 501.0709; found: 501.0715.

*4.1.4.7. N-(3-ethynylphenyl)-7-methoxy-6-(3-(2-nitro-1H-imidazol-1-yl)propoxy)quinazolin-4-amine (**15g**).* White solid, yield: 63%, mp: 209–211 °C. ^{1}H NMR (500 MHz, DMSO-d_6) δ 9.48 (s, 1H), 8.51 (s, 1H), 7.98 (t, J = 1.5 Hz, 1H), 7.90–7.86 (m, 1H), 7.84 (s, 1H), 7.69 (d, J = 1.0 Hz, 1H), 7.41 (t, J = 8.0 Hz, 1H), 7.23–7.20 (m, 2H), 7.19 (d, J = 1.0 Hz, 1H), 4.63 (t, J = 7.0 Hz, 2H), 4.29–4.15 (m, 3H), 3.94 (s, 3H), 2.45–2.35 (m, 2H). ^{13}C NMR (100 MHz, DMSO-d_6) δ 158.2, 156.5, 149.1, 148.5, 144.7, 137.2, 135.3, 129.3, 129.1, 127.9, 127.8 (2), 125.5, 121.9, 107.3, 105.3, 99.4, 82.9, 81.3, 67.1, 56.4, 46.9, 29.0. ESI-MS m/z: 445 $[M+H]^+$. HRMS (ESI): m/z calcd for $(C_{23}H_{20}N_6O_4 + H)^+$: 445.1624; found: 445.1633.

*4.1.4.8. N-(3-ethynylphenyl)-7-methoxy-6-(4-(2-nitro-1H-imidazol-1-yl)butoxy)quinazolin-4-amine (**15h**).* White solid, yield: 62%, mp: 207–209 °C. ^{1}H NMR (500 MHz, DMSO-d_6) δ 11.51 (s, 1H), 8.85 (s, 1H), 8.39 (s, 1H), 7.86 (s, 1H), 7.80–7.74 (m, 2H), 7.48 (t, J = 8.0 Hz, 1H), 7.42–7.38 (m, 1H), 7.33 (s, 1H), 7.18 (d, J = 0.5 Hz, 1H), 4.50 (t, J = 7.0 Hz, 2H), 4.32–4.23 (m, 3H), 3.97 (s, 3H), 2.03–1.94 (m, 2H), 1.86–1.78 (m, 2H). ^{13}C NMR (100 MHz, DMSO-d_6) δ 158.2, 156.5, 149.4, 148.6, 144.58, 137.3, 135.4, 129.3, 129.1, 128.0, 127.9, 127.7, 125.4, 122.0, 107.2, 105.0, 100.0, 82.9, 81.3, 69.2, 56.5, 49.1, 26.5, 25.2. ESI-MS m/z: 459 $[M+H]^+$. HRMS (ESI): m/z calcd for $(C_{24}H_{22}N_6O_4 + H)^+$: 459.1781; found: 459.1784.

*4.1.4.9. N-(3-ethynylphenyl)-7-methoxy-6-((5-(2-nitro-1H-imidazol-1-yl)pentyl)oxy)quinazolin-4-amine (**15i**).* White solid, yield: 64%, mp: 197–199 °C. ^{1}H NMR (500 MHz, DMSO-d_6) δ 11.29 (s, 1H),

8.84 (s, 1H), 8.26 (s, 1H), 7.84 (t, J = 2.0 Hz, 1H), 7.77–7.72 (m, 1H), 7.72 (d, J = 1.0 Hz, 1H), 7.49 (t, J = 8.0 Hz, 1H), 7.42–7.38 (m, 1H), 7.31 (s, 1H), 7.17 (d, J = 1.0 Hz, 1H), 4.42 (t, J = 7.5 Hz, 2H), 4.28 (s, 1H), 4.21 (t, J = 6.5 Hz, 2H), 3.98 (s, 3H), 1.91–1.82 (m, 4H), 1.51–1.41 (m, 2H). ^{13}C NMR (100 MHz, DMSO-d_6) δ 157.8, 156.1, 152.2, 149.3, 144.5, 138.9, 137.7, 129.1, 128.8, 127.9, 127.8, 127.2, 124.9, 122.0, 107.6, 104.3, 101.1, 83.0, 81.2, 69.2, 56.4, 49.3, 29.4, 27.9, 22.4. ESI-MS m/z: 473 $[M+H]^+$. HRMS (ESI): m/z calcd for $(C_{25}H_{24}N_6O_4 + H)^+$: 473.1937; found: 473.1947.

*4.1.4.10. N-(3-ethynylphenyl)-7-methoxy-6-((6-(2-nitro-1H-imidazol-1-yl)hexyl)oxy)quinazolin-4-amine (**15j**).* White solid, yield: 57%, mp: 174–176 °C. ^{1}H NMR (400 MHz, DMSO-d_6) δ 9.46 (s, 1H), 8.50 (s, 1H), 7.99 (t, J = 1.6 Hz, 1H), 7.92–7.87 (m, 1H), 7.82 (s, 1H), 7.70 (d, J = 0.8 Hz, 1H), 7.40 (t, J = 8.0 Hz, 1H), 7.23–7.19 (m, 2H), 7.18 (d, J = 0.8 Hz, 1H), 4.40 (t, J = 7.2 Hz, 2H), 4.20 (s, 1H), 4.14 (t, J = 6.4 Hz, 2H), 3.94 (s, 3H), 1.89–1.79 (m, 4H), 1.58–1.47 (m, 2H), 1.45–1.35 (m, 2H). ^{13}C NMR (100 MHz, DMSO-d_6) δ 156.3, 154.6, 152.9, 148.5, 147.1, 144.7, 140.0, 129.1, 128.0 (2), 126.5, 125.0, 122.8, 121.9, 109.1, 107.5, 102.6, 83.7, 80.8, 68.8, 56.0, 49.5, 29.9, 28.7, 25.8, 25.3. ESI-MS m/z: 487 $[M+H]^+$. HRMS (ESI): m/z calcd for $(C_{26}H_{26}N_6O_4 + H)^+$: 487.2094; found: 487.2103.

*4.1.4.11. N-(3-chloro-4-((3-fluorobenzyl)oxy)phenyl)-7-methoxy-6-(3-(2-nitro-1H-imidazol-1-yl)propoxy) quinazolin-4-amine (**15k**).* White solid, yield: 43%, mp: 168–170 °C. ^{1}H NMR (500 MHz, DMSO-d_6) δ 9.40 (s, 1H), 8.46 (s, 1H), 7.94 (d, J = 2.5 Hz, 1H), 7.80 (s, 1H), 7.72–7.64 (m, 2H), 7.52–7.43 (m, 1H), 7.36–7.30 (m, 2H), 7.27 (d, J = 9.0 Hz, 1H), 7.22–7.15 (m, 3H), 5.25 (s, 2H), 4.63 (t, J = 7.0 Hz, 2H), 4.19 (t, J = 5.5 Hz, 2H), 3.93 (s, 3H), 2.44–2.32 (m, 2H). ^{13}C NMR (100 MHz, DMSO-d_6) δ 162.18 (d, J_{C-F} = 243.6 Hz), 156.2, 154.4, 152.9, 149.4, 147.8, 147.0, 144.7, 139.7 (d, J_{C-F} = 7.4 Hz), 133.5, 130.5 (d, J_{C-F} = 8.2 Hz), 127.9, 127.8, 123.9, 123.3 (d, J_{C-F} = 2.8 Hz), 122.1, 121.0, 114.7 (d, J_{C-F} = 21.0 Hz), 114.3, 114.0 (d, J_{C-F} = 21.9 Hz), 108.6, 107.3, 102.9, 69.4 (d, J_{C-F} = 1.0 Hz), 66.0, 55.8, 47.0, 29.1. ESI-MS m/z: 579 $[M+H]^+$. HRMS (ESI): m/z calcd for $(C_{28}H_{24}ClFN_6O_5 + H)^+$: 579.1559; found: 579.1565.

*4.1.4.12. N-(3-chloro-4-((3-fluorobenzyl)oxy)phenyl)-7-methoxy-6-(4-(2-nitro-1H-imidazol-1-yl)butoxy)quinazolin-4-amine (**15l**).* White solid, yield: 45%, mp: 146–148 °C. ^{1}H NMR (400 MHz, DMSO-d_6) δ 9.41 (s, 1H), 8.45 (s, 1H), 7.94 (d, J = 2.8 Hz, 1H), 7.80 (s, 1H), 7.77 (d, J = 1.2 Hz, 1H), 7.72–7.66 (m, 1H), 7.51–7.44 (m, 1H), 7.36–7.29 (m, 2H), 7.27 (d, J = 9.2 Hz, 1H), 7.21 (d, J = 1.2 Hz, 1H), 7.20–7.15 (m, 2H), 5.25 (s, 2H), 4.52 (t, J = 6.8 Hz, 2H), 4.18 (t, J = 6.0 Hz, 2H), 3.93 (s, 3H), 2.08–1.95 (m, 2H), 1.89–1.78 (m, 2H). ^{13}C NMR (100 MHz, DMSO-d_6) δ 162.2 (d, J_{C-F} = 243.6 Hz), 156.2, 154.4, 152.8, 149.4, 148.0, 146.8, 144.6, 139.7 (d, J_{C-F} = 7.7 Hz), 133.5, 130.5 (d, J_{C-F} = 8.2 Hz), 127.9, 127.8 (d, J_{C-F} = 4.1 Hz), 124.0, 123.3 (d, J_{C-F} = 2.6 Hz), 122.1, 121.0, 114.7 (d, J_{C-F} = 20.7 Hz), 114.3, 114.0 (d, J_{C-F} = 21.9 Hz), 108.7, 107.3, 102.7, 69.4, 68.5, 55.8, 49.2, 26.7, 25.4. ESI-MS m/z: 593 $[M+H]^+$. HRMS (ESI): m/z calcd for $(C_{29}H_{26}ClFN_6O_5 + H)^+$: 593.1715; found: 593.1716.

*4.1.4.13. N-(3-chloro-4-((3-fluorobenzyl)oxy)phenyl)-7-methoxy-6-((5-(2-nitro-1H-imidazol-1-yl)pentyl)oxy)quinazolin-4-amine (**15m**).* White solid, yield: 48%, mp: 134–136 °C. ^{1}H NMR (400 MHz, DMSO-d_6) δ 9.41 (s, 1H), 8.44 (s, 1H), 7.94 (d, J = 2.8 Hz, 1H), 7.78 (s, 1H), 7.72 (d, J = 0.8 Hz, 1H), 7.70–7.67 (m, 1H), 7.51–7.44 (m, 1H), 7.36–7.30 (m, 2H), 7.27 (d, J = 9.2 Hz, 1H), 7.23–7.14 (m, 2H), 5.25 (s, 2H), 4.44 (t, J = 7.2 Hz, 2H), 4.13 (t, J = 6.4 Hz, 2H), 3.92 (s, 3H), 1.95–1.83 (m, 4H), 1.55–1.44 (m, 2H). ^{13}C NMR (100 MHz, DMSO-d_6) δ 162.2 (d, J_{C-F} = 243.6 Hz), 156.2, 154.3, 152.8, 149.4, 148.2, 146.8, 144.5, 139.7 (d, J_{C-F} = 7.4 Hz), 133.5, 130.5 (d, J_{C-F} = 8.2 Hz), 127.9, 127.8, 124.0, 123.3 (d, J_{C-F} = 2.7 Hz, 1H), 122.2, 121.0, 114.7 (d, J_{C-F} = 21.1 Hz), 114.3, 114.0 (d, J_{C-F} = 21.8 Hz), 108.7, 107.2, 102.5, 69.4 (d, J_{C-F} = 1.1 Hz), 68.5, 55.8, 49.3, 29.5, 28.1, 22.5. ESI-MS m/z: 607 $[M+H]^+$. HRMS (ESI): m/z calcd for $(C_{30}H_{28}ClFN_6O_5 + H)^+$: 607.1872; found: 607.1879.

*4.1.4.14. N-(3-chloro-4-((3-fluorobenzyl)oxy)phenyl)-7-methoxy-6-((6-(2-nitro-1H-imidazol-1-yl)hexyl)oxy)quinazolin-4-amine (**15n**).* White solid, yield: 51%, mp: 123–125 °C. ^{1}H NMR (400 MHz, DMSO-d_6) δ 9.41 (s, 1H), 8.45 (s, 1H), 7.94 (d, J = 2.8 Hz, 1H), 7.78 (s, 1H), 7.73–7.66 (m, 2H), 7.50–7.45 (m, 1H), 7.36–7.29 (m, 2H), 7.27 (d, J = 9.2 Hz, 1H), 7.22–7.14 (m, 3H), 5.25 (s, 2H), 4.40 (t, J = 7.2 Hz, 2H), 4.12 (t, J = 6.4 Hz, 2H), 3.93 (s, 3H), 1.90–1.78 (m, 4H),1.56–1.48 (m, 2H), 1.44–1.35 (m, 2H). ^{13}C NMR (100 MHz, DMSO-d_6) δ 162.2 (d, J_{C-F} = 243.6 Hz), 156.2, 154.3, 152.8, 149.4, 148.2, 146.7, 144.5, 139.7 (d, J_{C-F} = 7.4 Hz), 133.5, 130.5 (d, J_{C-F} = 8.1 Hz), 127.8 (2), 124.0, 123.3 (d, J_{C-F} = 2.7 Hz), 122.2, 121.0, 114.7 (d, J_{C-F} = 20.9 Hz), 114.3, 114.0 (d, J_{C-F} = 21.8 Hz), 108.7, 107.2, 102.4, 69.4, 68.6, 55.8, 49.3, 29.7, 28.5, 25.6, 25.1. ESI-MS m/z: 621 $[M+H]^+$. HRMS (ESI): m/z calcd for $(C_{31}H_{30}ClFN_6O_5 + H)^+$: 621.2028; found: 621.2029.

*4.1.4.15. N-(3-chloro-4-fluorophenyl)-7-methoxy-6-(2-(2-methyl-5-nitro-1H-imidazol-1-yl)ethoxy)quinazolin-4-amine (**15o**).* White solid, yield: 41%, mp: 244–246 °C. ^{1}H NMR (500 MHz, DMSO-d_6) δ 9.54 (s, 1H), 8.49 (s, 1H), 8.40 (s, 1H), 8.12–8.05 (m, 1H), 7.82 (s, 1H), 7.75 (d, J = 6.5 Hz, 1H), 7.44 (t, J = 9.0 Hz, 1H), 7.20 (s, 1H), 4.53 (t, J = 4.5 Hz, 2H), 4.44 (t, J = 4.5 Hz, 2H), 3.92 (s, 3H). ^{13}C NMR (100 MHz, DMSO-d_6) δ 156.1, 154.2, 153.2 (d, J_{C-F} = 242.8 Hz), 152.9, 152.0, 147.3 (2), 146.0, 145.4, 136.7 (d, J_{C-F} = 3.0 Hz), 123.4, 122.5, 122.2 (d, J_{C-F} = 6.7 Hz), 118.8 (d, J_{C-F} = 18.3 Hz), 116.6 (d, J_{C-F} = 21.7 Hz), 108.6, 107.5, 103.1, 67.8, 56.0, 45.8, 12.6. ESI-MS m/z: 473 $[M+H]^+$. HRMS (ESI): m/z calcd for $(C_{21}H_{18}ClFN_6O_4 + H)^+$: 473.1140; found: 473.1144.

*4.1.4.16. N-(3-chloro-4-fluorophenyl)-7-methoxy-6-(3-(2-methyl-5-nitro-1H-imidazol-1-yl)propoxy)-quinazolin-4-amine (**15p**).* White solid, yield: 44%, mp: 207–209 °C. ^{1}H NMR (500 MHz, DMSO-d_6) δ 9.56 (s, 1H), 8.50 (s, 1H), 8.41 (s, 1H), 8.12–8.08 (m, 1H), 7.80 (s, 1H), 7.79–7.71 (m, 1H), 7.44 (t, J = 9.0 Hz, 1H), 7.21 (s, 1H), 4.21 (t, J = 7.0 Hz, 2H), 4.14 (t, J = 5.5 Hz, 2H), 3.92 (s, 3H), 2.38–2.31 (m, 5H). ^{13}C NMR (100 MHz, DMSO-d_6) δ 156.1, 154.5, 153.2 (d, J_{C-F} = 242.9 Hz), 152.7, 147.8, 146.8, 145.5, 145.1, 136.7 (d, J_{C-F} = 2.5 Hz), 123.5, 122.3 (d, J_{C-F} = 6.8 Hz), 122.0, 118.8 (d, J_{C-F} = 18.4 Hz), 116.5 (d, J_{C-F} = 21.6 Hz), 108.6, 107.2, 102.9, 65.6, 55.9, 43.6, 28.9, 12.4. ESI-MS m/z: 487 $[M+H]^+$. HRMS (ESI): m/z calcd for $(C_{22}H_{20}ClFN_6O_4 + H)^+$: 487.1297; found: 487.1303.

*4.1.4.17. N-(3-chloro-4-fluorophenyl)-7-methoxy-6-(4-(2-methyl-5-nitro-1H-imidazol-1-yl)-butoxy)-quinazolin-4-amine (**15q**).* White solid, yield: 48%, mp: 158–160 °C. ^{1}H NMR (500 MHz, DMSO-d_6) δ 9.66 (s, 1H), 8.51 (s, 1H), 8.40 (s, 1H), 8.12–8.08 (m, 1H), 7.84 (s, 1H), 7.80–7.76 (m, 1H), 7.44 (t, J = 9.0 Hz, 1H), 7.20 (s, 1H), 4.19 (t, J = 6.0 Hz, 2H), 4.12 (t, J = 7.0 Hz, 2H), 3.94 (s, 3H), 2.38 (s, 3H), 2.01–1.91 (m, 2H), 1.87–1.75 (m, 2H). ^{13}C NMR (100 MHz, DMSO-d_6) δ 156.3, 154.8, 153.4 (d, J_{C-F} = 243.3 Hz), 152.0, 148.3, 145.3, 145.2, 144.9, 136.4 (d, J_{C-F} = 2.8 Hz), 123.9, 122.7 (d, J_{C-F} = 6.8 Hz), 122.1, 118.8 (d, J_{C-F} = 18.4 Hz), 116.5 (d, J_{C-F} = 21.6 Hz), 108.5, 106.1, 103.0, 68.6, 56.0, 46.1, 26.4, 25.2, 12.6. ESI-MS m/z: 501 $[M+H]^+$. HRMS (ESI): m/z calcd for $(C_{23}H_{22}ClFN_6O_4 + H)^+$: 501.1453; found: 501.1456.

*4.1.4.18. N-(3-bromophenyl)-7-methoxy-6-(3-(2-methyl-5-nitro-1H-imidazol-1-yl)propoxy)quinazolin-4-amine (**15r**).* White solid, yield: 49%, mp: 94–96 °C. ^{1}H NMR (500 MHz, DMSO-d_6) δ 9.47 (s, 1H), 8.51 (s, 1H), 8.40 (s, 1H), 8.12 (s, 1H), 7.84 (d, J = 8.0 Hz, 1H), 7.80 (s, 1H), 7.34 (t, J = 8.0 Hz, 1H), 7.26 (d, J = 8.0 Hz, 1H), 7.21 (s, 1H), 4.21

(t, J = 6.5 Hz, 2H), 4.15 (t, J = 5.5 Hz, 2H), 3.92 (s, 3H), 2.37–2.32 (m, 5H). ^{13}C NMR (100 MHz, DMSO-d_6) δ 155.9, 154.5, 152.8, 147.8, 147.2, 145.5, 145.1, 141.2, 130.4, 125.6, 124.0, 122.0, 121.2, 120.5, 108.8, 107.4, 102.9, 65.6, 55.9, 43.6, 28.9, 12.4. ESI-MS m/z: 515 $[M+H]^+$. HRMS (ESI): m/z calcd for $(C_{22}H_{21}BrN_6O_4 + H)^+$: 515.0865; found: 515.0871.

4.2. Pharmacology

Human colorectal adenocarcinoma HT-29 cells were purchased from Cell Bank of China Science Academy (Shanghai, China). The above cells were cultured in RPMI-1640 (Invitrogen Corp., Carlsbad, CA) medium with heat-inactivated 10% fetal bovine serum, penicillin (100 units/mL) and streptomycin (100 mg/mL) and incubated in hypoxic atmosphere with 2% O_2, 5% CO_2 and in normoxic atmosphere with 20% O_2, 5% CO_2 at 37 °C.

4.2.1. In vitro enzymatic activity assay

Wild type EGFR and the Z′-Lyte Kinase Kit were purchased from Invitrogen. Ten concentration gradients were set for all the tested compounds. The experiments were performed according to the instructions of the manufacturer.

4.2.2. Cytotoxicity assay

The cytotoxic activity *in vitro* was measured using sulforhodamin B (SRB) assay. All the compounds were dissolved in DMSO at the concentrations 10.0 mg/mL and were then diluted to the appropriate concentrations. Cells were plated in 96-well plates (5×10^3 per well) for 24 h and subsequently treated with different concentrations of all tested compounds under normoxia or hypoxia for 72 h, respectively. Cells were then washed with PBS and fixed with 10% (w/v) trichloroacetic acid at 4 °C for one hour. After washing, the cells were stained for 30 min with 0.4% SRB dissolved in 1% acetic acid. Then the cells were washed by 1% acetic acid for 5 times, and protein-bound dye was extracted with 10 mmol unbuffered Tris base. The absorbance was measured at 515 nm using a multiscan spectrum (Thermo Electron Co., Vantaa, Finland). The inhibition rate on cell proliferation of each well was calculated as (A515 control cells A515 treated cells)/A515 control cells × 100%, and the IC_{50} values were determined by Logit method.

4.3. Mimic the reductive activation of compound 15c

Compound **15c** (2.0 mg, 4.1 μmol) and cysteine (5.0 mg, 41.1 μmol) was firstly dissolved in 0.5 mL dimethyl sulfoxide and then added to 3 mL phosphate buffer saline (pH = 7.4, 50 μM), then Zn dust (6.7 mg, 102.7 μmol) and ammonium chloride (11.0 mg, 205.4 μmol) were added to the reaction mixture. The reaction flask was evacuated and backfilled with nitrogen three times. The reaction mixture was stirred at 37 °C under a nitrogen balloon for 12 h and then filtered through 0.45 μm microfiltration membrane and the filtrate was analyzed through HPLC-Q-ToF-MS (AB Sciex Triple TOF 5600+). The column was Eclipse Plus C18 (5 μm, 4.6 × 250 mm), the mobile phase was MeOH:H_2O (0.1% HCOOH + 5 mM $AcONH_4$) = 44:56 at the flow rate of 1.0 mL/min, and the detected wavelength was 330 nm, with column temperature at 30 °C.

4.4. Metabolic stability assay [21,32]

The assay mixtures contained the following substance with the indicated final concentrations: 50 mM potassium phosphate buffer (pH 7.4), 5 mM $MgCl_2$, microsomes (1 mg/mL) with or without 2 mM NADPH. The mixtures were preincubated at 37 °C both under normoxia (20% O_2, 5% CO_2) and hypoxia (2% O_2, 5% CO_2). The metabolism reaction was initiated by the addition of 5 μM test compound to the incubation mixtures. At 0 and 30 min, the reaction mixture was quenched with equal volume of acetonitrile containing 0.1% formic acid. The samples were centrifuged for 10 min at 10,000 *g*. The supernatant was transferred to a vial for HPLC analysis.

4.5. Molecular modeling

The EGFR-gefitinib protein–ligand complex crystal structure (PDB ID: 2ITY) was chosen as the template to study the docking mode of compound **15c** with EGFR. The molecular docking procedure was performed by using C-DOCKER protocol within Discovery Studio 2.1. For ligand preparation, the 3D structure of compound **15c** was generated and minimized. For enzyme preparation, the hydrogen atoms were added, and the CHARMm force field was employed. The whole EGFR enzyme was defined as a receptor and the site sphere was selected based on the ligand binding location of gefitinib, then gefitinib was removed and compound **15c** was placed during the molecular docking procedure. Types of interactions of the docked enzyme with ligand were analyzed after end of molecular docking. Ten docking poses were saved for each ligand and the final docked conformation was scored and selected based on calculated C-DOCKER-energy.

Acknowledgments

We thank the support of the National Natural Science Foundation of China (81072575). We thank Dr. Ke Ding (Guangzhou Institutes of Biomedicine and Health, Chinese Academy of Sciences) for performing the EGFR activity evaluation. We also thank Mrs Jianyang Pan (Pharmaceutical Informatics Institute, Zhejiang University) for performing the NMR and MS spectrometry tests and Mrs Xiaodan Wu (Analysis Center of Agrobiology and Environmental Sciences, Zhejiang University) for performing the HPLC-Q-ToF-MS test.

References

[1] N.E. Hynes, H.A. Lane, ERBB receptors and cancer: the complexity of targeted inhibitors, Nat. Rev. Cancer 5 (2005) 341–354.
[2] R.L. Rego, N.R. Foster, T.C. Smyrk, M. Le, M.J. O'Connell, D.J. Sargent, H. Windschitl, F.A. Sinicrope, Prognostic effect of activated EGFR expression in human colon carcinomas: comparison with EGFR status, Br. J. Cancer 102 (2010) 165–172.
[3] C. Cao, S. Lu, A. Sowa, R. Kivlin, A. Amaral, W.M. Chu, H. Yang, W. Di, Y.S. Wan, Priming with EGFR tyrosine kinase inhibitor and EGF sensitizes ovarian cancer cells to respond to chemotherapeutical drugs, Cancer Lett. 266 (2008) 249–262.
[4] T. Mitsudomi, Y. Yatabe, Epidermal growth factor receptor in relation to tumor development: EGFR gene and cancer, Febs J. 277 (2010) 301–308.
[5] R. Patel, H.Y. Leung, Targeting the EGFR-family for therapy: biological challenges and clinical perspective, Curr. Pharm. Des. 18 (2012) 2672–2679.
[6] W.R. Wilson, M.P. Hay, Targeting hypoxia in cancer therapy, Nat. Rev. Cancer 11 (2011) 393–410.
[7] T. Wang, T. Niki, A. Goto, S. Ota, T. Morikawa, Y. Nakamura, E. Ohara, S. Ishikawa, H. Aburatani, J. Nakajima, M. Fukayama, Hypoxia increases the motility of lung adenocarcinoma cell line A549 via activation of the epidermal growth factor receptor pathway, Cancer Sci. 98 (2007) 506–511.
[8] H. Nishi, K.H. Nishi, A.C. Johnson, Early growth response-1 gene mediates up-regulation of epidermal growth factor receptor expression during hypoxia, Cancer Res. 62 (2002) 827–834.
[9] G.C. Lancini, E. Lazzari, V. Arioli, P. Bellani, Synthesis relationship between structure and activity of 2-nitroimidazole derivatives, J. Med. Chem. 12 (1969) 775–780.
[10] M.B. Noss, R. Panicucci, R.A. McClelland, A.M. Rauth, 1-Methyl-2-nitrosoimidazole – cytotoxic and glutathione depleting capabilities, Int. J. Radiat. Oncol. 16 (1989) 1015–1019.
[11] L. Hoigebazar, J.M. Jeong, J.Y. Lee, D. Shetty, B.Y. Yang, Y.S. Lee, D.S. Lee, J.K. Chung, M.C. Lee, Syntheses of 2-nitroimidazole derivatives conjugated with 1,4,7-triazacyclononane-*N*,*N*′-diacetic acid labeled with F-18 using an aluminum complex method for hypoxia imaging, J. Med. Chem. 55 (2012) 3155–3162.

[12] P. Kumar, G. Shustov, H. Liang, V. Khlebnikov, W.Z. Zheng, X.H. Yang, C. Cheeseman, L.I. Wiebe, Design, synthesis, and preliminary biological evaluation of 6-*O*-glucose-azomycin adducts for diagnosis and therapy of hypoxic tumors, J. Med. Chem. 55 (2012) 6033–6046.
[13] J. van Loon, M.H.M. Janssen, M. Ollers, H. Aerts, L. Dubois, M. Hochstenbag, A.M.C. Dingemans, R. Lalisang, B. Brans, B. Windhorst, G.A. van Dongen, H. Kolb, J. Zhang, D. De Ruysscher, P. Lambin, PET imaging of hypoxia using F-18 HX4: a phase I trial, Eur. J. Nucl. Med. Mol. Imaging 37 (2010) 1663–1668.
[14] C.H. Yun, T.J. Boggon, Y.Q. Li, M.S. Woo, H. Greulich, M. Meyerson, M.J. Eck, Structures of lung cancer-derived EGFR mutants and inhibitor complexes: mechanism of activation and insights into differential inhibitor sensitivity, Cancer Cell 11 (2007) 217–227.
[15] J. Stamos, M.X. Sliwkowski, C. Eigenbrot, Structure of the epidermal growth factor receptor kinase domain alone and in complex with a 4-anilinoquinazoline inhibitor, J. Biol. Chem. 277 (2002) 46265–46272.
[16] E.R. Wood, A.T. Truesdale, O.B. McDonald, D. Yuan, A. Hassell, S.H. Dickerson, B. Ellis, C. Pennisi, E. Horne, K. Lackey, K.J. Alligood, D.W. Rusnak, T.M. Gilmer, L. Shewchuk, A unique structure for epidermal growth factor receptor bound to GW572016 (Lapatinib): relationships among protein conformation, inhibitor off-rate, and receptor activity in tumor cells, Cancer Res. 64 (2004) 6652–6659.
[17] F. Solca, G. Dahl, A. Zoephel, G. Bader, M. Sanderson, C. Klein, O. Kraemer, F. Himmelsbach, E. Haaksma, G.R. Adolf, Target binding properties and cellular activity of afatinib (BIBW 2992), an irreversible erbb family blocker, J. Pharmacol. Exp. Ther. 343 (2012) 342–350.
[18] V. Chandregowda, A.K. Kush, G.C. Reddy, Synthesis and in vitro antitumor activities of novel 4-anilinoquinazoline derivatives, Eur. J. Med. Chem. 44 (2009) 3046–3055.
[19] S.H. Chang, L.W. Zhang, S.L. Xu, J.F. Luo, X.Y. Lu, Z. Zhang, T.F. Xu, Y.X. Liu, Z.C. Tu, Y. Xu, X.M. Ren, M.Y. Geng, J. Ding, D.Q. Pei, K. Ding, Design, synthesis, and biological evaluation of novel conformationally constrained inhibitors targeting epidermal growth factor receptor threonine(790)→methionine(790) mutant, J. Med. Chem. 55 (2012) 2711–2723.
[20] R.F. Borch, J.W. Liu, J.P. Schmidt, J.T. Marakovits, C. Joswig, J.J. Gipp, R.T. Mulcahy, Synthesis and evaluation of nitroheterocyclic phosphoramidates as hypoxia-selective alkylating agents, J. Med. Chem. 43 (2000) 2258–2265.
[21] J.X. Duan, H. Jiao, J. Kaizerman, T. Stanton, J.W. Evans, L. Lan, G. Lorente, M. Banica, D. Jung, J.W. Wang, H.Y. Ma, X.M. Li, Z.J. Yang, R.M. Hoffman, W.S. Ammons, C.P. Hart, M. Matteucci, Potent and highly selective hypoxia-activated achiral phosphoramidate mustards as anticancer drugs, J. Med. Chem. 51 (2008) 2412–2420.
[22] M.P. Hay, F.B. Pruijn, S.A. Gamage, H.D.S. Liyanage, M.S. Kovacs, A.V. Patterson, W.R. Wilson, J.M. Brown, W.A. Denny, DNA-targeted 1,2,4-benzotriazine 1,4-dioxides: potent analogues of the hypoxia-selective cytotoxin tirapazamine, J. Med. Chem. 47 (2004) 475–488.
[23] S. Maya, B. Sarmento, V.K. Lakshmanan, D. Menon, R. Jayakumar, Actively targeted cetuximab conjugated gamma-poly(glutamic acid)-docetaxel nanomedicines for epidermal growth factor receptor over expressing colon cancer cells, J. Biomed. Nanotechnol. 10 (2014) 1416–1428.
[24] M.V. Papadopoulou, W.D. Bloomer, Exploiting hypoxia in solid tumors with DNA-targeted bioreductive drugs, Drug. Future 29 (2004) 807–819.
[25] A.J. Varghese, G.F. Whitmore, Misonidazole-glutathione conjugates in CHO cells, Int. J. Radiat. Oncol. 10 (1984) 1341–1345.
[26] H. Nagasawa, Y. Uto, K.L. Kirk, H. Hori, Design of hypoxia-targeting drugs as new cancer chemotherapeutics, Biol. Pharm. Bull. 29 (2006) 2335–2342.
[27] A.J. Varghese, G.F. Whitmore, Properties of 2-hydroxylaminoimidazoles and their implications for the biological effects of 2-nitroimidazoles, Chem. Biol. Interact. 56 (1985) 269–287.
[28] C. Carmi, E. Galvani, F. Vacondio, S. Rivara, A. Lodola, S. Russo, S. Aiello, F. Bordi, G. Costantino, A. Cavazzoni, R.R. Alfieri, A. Ardizzoni, P.G. Petronini, M. Mor, Irreversible inhibition of epidermal growth factor receptor activity by 3-aminopropanamides, J. Med. Chem. 55 (2012) 2251–2264.
[29] V.S. Gopinath, J. Pinjari, R.T. Dere, A. Verma, P. Vishwakarma, R. Shivahare, M. Moger, P.S.K. Goud, V. Ramanathan, P. Bose, M.V.S. Rao, S. Gupta, S.K. Puri, D. Launay, D. Martin, Design, synthesis and biological evaluation of 2-substituted quinolines as potential antileishmanial agents, Eur. J. Med. Chem. 69 (2013) 527–536.
[30] L. Kumar, A. Sarswat, N. Lal, V.L. Sharma, A. Jain, R. Kumar, V. Verma, J.P. Maikhuri, A. Kumar, P.K. Shukla, G. Gupta, Imidazole derivatives as possible microbicides with dual protection, Eur. J. Med. Chem. 45 (2010) 817–824.
[31] P. Kowalski, K. Nowak, B. Szpakiewicz, Synthesis and prediction of bioactivity of new nitroimidazole derivatives, J. Heterocycl. Chem. 42 (2005) 883–888.
[32] M.V. Papadopoulou, M. Ji, M.K. Rao, W.D. Bloomer, Reductive metabolism of the nitroimidazole-based hypoxia-selective cytotoxin NLCQ-1 (NSC 709257), Oncol. Res. 14 (2003) 21–29.